

The influence of placental metabolism on fatty acid transfer to the fetus^S

Simone Perazzolo,^{*,†} Birgit Hirschmugl,[§] Christian Wadsack,[§] Gernot Desoye,[§]
Rohan M. Lewis,^{1,†,**,†} and Bram G. Sengers^{1,2,*,†}

Faculty of Engineering and Environment,^{*} Bioengineering Research Group, Faculty of Medicine,^{**} and Institute for Life Sciences Southampton,[†] University of Southampton, SO17 1BJ, UK; and Department of Obstetrics and Gynecology,[§] Medical University of Graz, 8036 Graz, Austria

Abstract The factors determining fatty acid transfer across the placenta are not fully understood. This study used a combined experimental and computational modeling approach to explore placental transfer of nonesterified fatty acids and identify the rate-determining processes. Isolated perfused human placenta was used to study the uptake and transfer of ¹³C-fatty acids and the release of endogenous fatty acids. Only 6.2 ± 0.8% of the maternal ¹³C-fatty acids taken up by the placenta was delivered to the fetal circulation. Of the unlabeled fatty acids released from endogenous lipid pools, 78 ± 5% was recovered in the maternal circulation and 22 ± 5% in the fetal circulation. Computational modeling indicated that fatty acid metabolism was necessary to explain the discrepancy between uptake and delivery of ¹³C-fatty acids. Without metabolism, the model overpredicts the fetal delivery of ¹³C-fatty acids 15-fold. Metabolic rate was predicted to be the main determinant of uptake from the maternal circulation. The microvillous membrane had a greater fatty acid transport capacity than the basal membrane. **■** This study suggests that incorporation of fatty acids into placental lipid pools may modulate their transfer to the fetus. Future work needs to focus on the factors regulating fatty acid incorporation into lipid pools.—Perazzolo, S., B. Hirschmugl, C. Wadsack, G. Desoye, R. M. Lewis, and B. G. Sengers. **The influence of placental metabolism on fatty acid transfer to the fetus.** *J. Lipid Res.* 2017. 58: 443–454.

Supplementary key words placenta • fatty acids • placental transport • dual placental perfusion • lipid computational model • compartmental modelling

Long-chain fatty acids are essential for the development of the fetal brain and visual system and as biosynthetic precursors for hormones (1). Impaired placental delivery of fatty acids to the fetus may result in developmental changes,

with consequences for the life-long health of the offspring (2). The mechanisms of fatty acid transfer to the fetus and which of these mechanisms is likely to be rate determining are not fully understood. In this study, placental fatty acid transfer was investigated using placental perfusion in combination with computational modeling.

The low solubility of fatty acids means that they are typically bound to carrier proteins (e.g., lipoproteins, albumin in plasma, and specific fatty acid binding proteins within the cytosol). Plasma albumin concentrations have been shown to be an important determinant of placental fatty acid transfer (3). Within the cytosol, fatty acid binding proteins in the placenta include the heart type and the liver type (4) to facilitate the cytosolic transfer (5). Fatty acids transfer across the human placenta and follow an overall concentration gradient, with concentrations higher in maternal plasma than in the fetal capillaries (6).

Between the maternal and the fetal blood, the syncytiotrophoblast layer of the villous tree is considered the primary barrier to nutrients transfer through the human placenta (6, 7). Membrane transport of fatty acids may occur by both simple (8) and facilitated diffusion (9). The relative contribution of simple and facilitated diffusion of fatty acids is disputed, but fatty acid transporters are found in the maternal-facing microvillous plasma membrane (MVM) of the syncytiotrophoblast and in the fetal-facing basal membrane (BM) (10). These membrane transporters include members of the fatty acid transport protein family, the fatty acid binding protein plasma membrane, and the fatty acid translocase/CD36 (11).

Membrane transport of nutrients is widely believed to be a rate-determining step in their transfer, but in the heart, it has been proposed that fatty acid uptake is determined by metabolic rate within the cell (12). The first step in fatty acid metabolism is conversion to acyl-CoA. This is mediated

This work was supported by the European Union's Seventh Framework Programme (FP7/2007-2013), project Early Nutrition under grant agreement 289346; by the Institute of Life Sciences, Southampton and EPSRC DTP (S.P.); and by the Austrian Science Fund FWF (W1241) and the Medical University of Graz through the PhD Program Molecular Fundamentals of Inflammation (DK-MOLIN) (B.H.). Data supporting this study are available at <http://doi.org/10.5258/SOTON/404179>

Manuscript received 6 October 2016 and in revised form 17 November 2016.

Published, *JLR Papers in Press*, December 2, 2016
DOI 10.1194/jlr.P072355

¹These authors contributed equally to the work.

²To whom correspondence should be addressed.

e-mail: B.G.Sengers@soton.ac.uk

S The online version of this article (available at <http://www.jlr.org>) contains a supplement.

by long-chain fatty acid acyl-CoA synthetase in the cytosol or, for the fatty acid transport protein family of membrane transporters, is directly associated with the membrane transport protein (13, 14). Acyl-CoA can then be esterified into different lipid pools, triglycerides, phospholipids, and cholesterol esters (15, 16); enter the β -oxidation pathway (17, 18); or be used for the biosynthesis of eicosanoids (19). Because most fatty acids are converted to Acyl-CoA in the cytosol, the fatty acid concentration would be expected to be low. Placental metabolism poses a problem for fatty acid transfer because acyl-CoA and its products cannot easily be released to the fetal circulation. This is analogous to an unresolved problem with placental glucose transfer because glucose is normally converted to glucose-6-phosphate as soon as it enters the cell trapping it there (20). Glucose transferred to the placenta must somehow bypass this process because there is no placental glucose-6-phosphatase. However, the placenta does express genes for enzymes that can release fatty acids from acyl-CoA, triglyceride, and phospholipid pools (18, 21). It has been suggested that glucose and fatty acid transfer may occur preferentially in regions of vascular syncytial membrane where diffusion distance is low and metabolism may be limited (22).

Compartmental modeling has provided insight into the placental transfer of amino acids, in particular by highlighting the role of amino acid metabolism (23–25). Similarly, mathematical modeling could help interpret the factors that affect fatty acid transfer because it is currently not clear which of these is rate determining. The aim of this study was to identify and evaluate the main factors that determine fatty acid transfer across the placenta by combining ex vivo placental perfusion experiments and computational modeling of the resulting data.

MATERIALS AND METHODS

Placental ex vivo perfusion

Healthy women with uncomplicated pregnancies were asked to participate in this study prior to elective caesarean sections. All women provided written informed consent, and the study was approved by the ethics committee of the Medical University of Graz (EK No. 24-529 ex 11/12).

For the six healthy placentas perfused in this study, maternal BMI was (mean and SEM) 28.4 ± 10.6 kg/m², placental weight was 665 ± 83 g, and gestation length was 38.8 ± 0.4 weeks.

The perfusion method used in this study was previously described by Schneider et al. (26). Briefly, within 20 min after delivery each placenta was examined in order to find a single intact cotyledon. The corresponding artery and vein pair, supplying the cotyledon, was cannulated, and the cotyledon was flushed immediately with prewarmed perfusion medium. The perfusion medium consists of phenol red free DMEM of 1g/l glucose (Gibco) and Earl's buffer of 116.4 mmol/l NaCl, 5.4 mmol/l KCl, 1.2 mmol/l NaH₂PO₄, 0.8 mmol/l MgSO₄·7 H₂O, 1.8 mmol/l CaCl₂, 26.2 mmol/l NaHCO₃ mixed in a 3:1 ratio (Merck, Darmstadt, Germany); 250 mg/l amoxicillin (Sigma-Aldrich, Steinheim, Germany); 10 g/l dextran FP40 (Serva, Heidelberg, Germany); a total

concentration of 11.1 mmol/l glucose (Merck); and 5 g/l essentially fatty acid-free BSA (Sigma-Aldrich, Seinhelm, Germany).

The cannulated cotyledon was placed in the preheated (37°C) perfusion chamber, and the fetal circulation flow rate was set to 4 ml/min. Thereafter, the maternal circulation was established at a flow rate of 8.4 ml/min, and both circulations were kept in the open circuit mode for 30 min. The maternal reservoir was changed to 200 ml perfusion medium containing 0.5% essential fatty acid-free BSA (Sigma-Aldrich, Schnellendorf, Germany) and ¹³C-fatty acid (37.2 μ M 16:0, 40.5 μ M 18:1, 1.6 μ M 18:2 n6) (Sigma-Aldrich, Schnellendorf, Germany) and unlabeled fatty acids (0.78 μ M 20:4 n6, 0.2 μ M 20:5 n3) (Sigma-Aldrich, Schnellendorf, Germany). The fetal circulation contained 0.5% BSA as an acceptor for fatty acids and was kept in open-circuit mode throughout the experiment. The maternal perfusate was recirculated for 180 min. Samples were taken from maternal artery and vein and from the fetal vein at 0, 10, 20, 30, 60, 90, 120, 150, and 180 min. The maternal reservoir was changed to perfusion medium containing 0.5% BSA, and both circulations were kept open during this washout phase. Sample collection was performed at 0, 10, 20, and 30 min during the washout phase. After removal of red blood cells, the samples were stored at -80°C until analysis.

Fatty acid analysis by GC/MS

Lipid extracts from samples collected during the perfusion experiment were extracted according to the method previously described by Matyash et al. (27). Nonesterified fatty acids were determined by Trace-DSQ GC/MS (Thermo Fisher Scientific, Waltham, MA) on electron impact MS mode, as previously published by Fuchs et al. (28).

The model development, parameter sensitivity, and analysis of transfer mechanisms were first performed using data from an initial experiment with 90 min of ¹³C-fatty acid infusion followed by a 30 min washout. Once the computational model was derived for this case, the same modeling methodology was applied to estimate the model parameters based on the data from the 180 min ¹³C-fatty acid infusion + 30 min washout experiments (n = 6).

Uptake and delivery mass balance

Mass balance calculations for the placental system were carried out using the experimental concentration data. Thus, for ¹³C-fatty acid:

$$u = \int_0^{T_{\text{perf}}} (c_{ma} - c_{mv}) Q_M dt \quad (\text{Eq. 1})$$

$$d = \int_0^{T_{\text{perf}}} c_{fv} Q_F dt \quad (\text{Eq. 2})$$

where u is the uptake by the placenta from the maternal circulation; d is the amount of fatty acid delivered to the fetal circulation (fetal delivery); c (μ mol/l) is the measured concentration; ma , mv , and fv refer to the experimental maternal artery, maternal vein, and the fetal vein measurements sampled over time, respectively. $T_{\text{perf}} = 180$ min is the experimental ¹³C-fatty acid perfusion time for the six experiments. The mass balance for ¹³C-fatty acid is $b_{\text{ra}} = u - d$. If $b = 0$, the entire amount of ¹³C-fatty acid taken up by the placenta was delivered to the fetal circulation. If $b > 0$, a certain amount of ¹³C-fatty acid was taken up by the placenta but not delivered to the fetal circulation and thus had to be retained by

the placenta. For the endogenous fatty acids, the net release from the tissue was estimated as the sum of the amount of fatty acids recovered in the maternal reservoir and the amount of fatty acids recovered in the fetal efflux: $b_{endo} = d - u$. Thus, when $b > 0$, a certain amount of endogenous fatty acid was released by the placental tissue.

Mathematical modeling

Based on the placental physiology and experimental setup, the main compartments involved in fatty acid transfer included in the model were (in order from maternal to fetal circulation) the experimental maternal reservoir R , the placental maternal intervillous space M , the syncytiotrophoblast fatty acid pool S (i.e., those intracellular fatty acids available for transport), and the fetoplacental capillaries F . Connected to S , an additional compartment P was added to account for the placental metabolism (Fig. 1). The placental metabolism represented all metabolic pathways that may occur in the placental tissue, including reversible and irreversible processes. We will refer to P and the placental metabolism as described here as the “metabolic pool.” This pool represents the sum of fatty acids that have been subject to metabolic processes, including esterification (into triglyceride, phospholipid, and cholesteryl-ester pools) and irreversible loss such as biosynthesis of eicosanoid or β -oxidation. The model configuration was based on current understanding of maternal-to-fetal transfer of fatty acids (29). The volume of each compartment was assumed constant and well mixed. Concentrations in the model were defined in accordance with the measured data, representing both unbound fatty acids and those bound to carriers. The placental metabolism was assumed to occur in the syncytiotrophoblast cytosol. The resulting model is described by the following set of governing equations:

$$\frac{dC_R}{dt} = \frac{1}{V_R}(-Q_M C_R + Q_M C_M) \quad (Eq. 3)$$

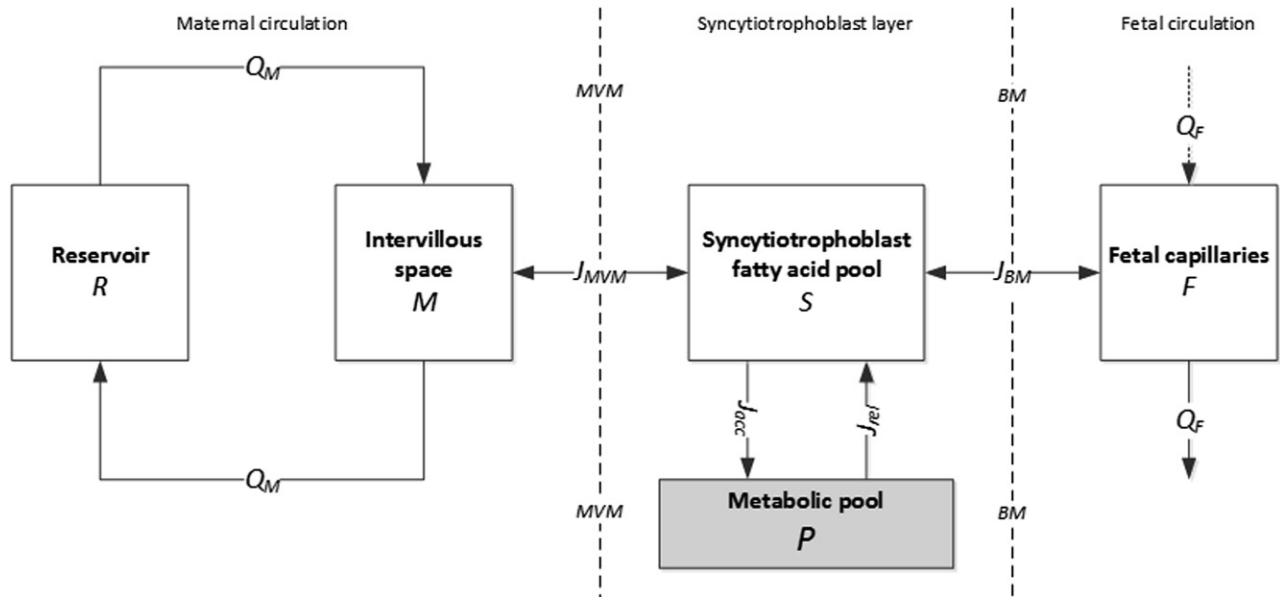


Fig. 1. Compartmental model schematic for fatty acid transfer across the placenta. R is the maternal reservoir; M is the maternal intervillous space; S is the syncytiotrophoblast fatty acid pool (intracellular fatty acids available for transport) and P is the metabolic pool, both contained in the syncytiotrophoblast volume; and F is the fetal compartment of the placenta, representing the fetal capillary volume. The maternal circulation was perfused in closed circuit with flow $Q_M = 8.4$ ml/min. J_{MVM} and J_{BM} ($\mu\text{mol}/\text{min}$) are the net fluxes across the placental membranes MVM and BM, respectively. J_{acc} and J_{rel} ($\mu\text{mol}/\text{min}$) are the metabolic fluxes representing the accumulation and release due to placental metabolism. The fetal circulation was perfused in an open circuit with flow $Q_F = 4$ ml/min.

$$\frac{dC_M}{dt} = \frac{1}{V_M}(Q_M C_R - Q_M C_M - J_{MVM}) \quad (Eq. 4)$$

$$\frac{dC_S}{dt} = \frac{1}{V_S}(J_{MVM} - J_{BM} - J_{acc} + J_{rel}) \quad (Eq. 5)$$

$$\frac{dC_P}{dt} = \frac{1}{V_P}(J_{acc} - J_{rel}) \quad (Eq. 6)$$

$$\frac{dC_F}{dt} = \frac{1}{V_F}(-Q_F C_F + Q_F C_{F,inp} + J_{BM}) \quad (Eq. 7)$$

Concentrations C ($\mu\text{mol}/\text{l}$) and volumes V (liters) of the compartments are indicated with the relevant subscripts (with $V_P = V_S$). $C_{F,inp}$ is the fetal umbilical artery input concentration, which was zero in the experiments. Q_M (l/min) is the maternal circulation flow. Q_F (l/min) is the fetal circulation flow. J_{MVM} ($\mu\text{mol}/\text{min}$) and J_{BM} ($\mu\text{mol}/\text{min}$) are the net fluxes across the MVM and BM, respectively. J_{acc} ($\mu\text{mol}/\text{min}$) and J_{rel} ($\mu\text{mol}/\text{min}$) are the fluxes of fatty acids from the pool S to the metabolic pool (accumulation pathway) and from the metabolic pool back to pool S (release pathway), respectively.

Membrane transport model

The membrane fluxes J_{MVM} and J_{BM} were modeled to represent a saturable bidirectional process. All different transport mechanisms, including dissociation and binding steps, were lumped together in a single “apparent” transport process. For the sake of simplicity, each fatty acid was considered independently (i.e., without an explicit model of competition). The same functional form was assumed on both MVM and BM, as follows (30):

$$J_{MVM} = v_{MVM} \left(\frac{C_M}{K_{MVM} + C_M} - \frac{C_S}{K_{MVM} + C_S} \right) \quad (\text{Eq. } 8)$$

$$J_{BM} = v_{BM} \left(\frac{C_S}{K_{BM} + C_S} - \frac{C_F}{K_{BM} + C_F} \right) \quad (\text{Eq. } 9)$$

The parameters v_{MVM} and v_{BM} ($\mu\text{mol}/\text{min}$) represent the maximum flux capacity of the respective membrane. K_{MVM} and K_{BM} ($\mu\text{mol}/\text{l}$) are the fatty acid dissociation constants for each membrane, with $K_{MVM} = K_{BM} = K$. Note that for $K \gg C$ this function reduces to a simple diffusive process. Thus, the fluxes are consistent with the concentration gradient: when $J_{MVM} > 0$ the net flux goes from M to S ; when $J_{BM} > 0$ the net flux goes from S to F .

Metabolic pool model

The metabolism fluxes J_{acc} and J_{rel} representing an enzymatic cascade, were approximated as a single “apparent” metabolic process with Michaelis-Menten kinetics. Thus:

$$J_{acc} = \frac{V_{max,acc} C_S}{K_{m,acc} + C_S} \quad (\text{Eq. } 10)$$

$$J_{rel} = \frac{V_{max,rel} C_P}{K_{m,rel} + C_P} \quad (\text{Eq. } 11)$$

where V_{max} and K_m are the Michaelis-Menten parameters. For the sake of simplicity, $K_{m,acc} = K_{m,rel} = K_m$, assuming that accumulation into the metabolic pool and release from the metabolic pool had the same apparent kinetics. An estimate for K_m was $435 \mu\text{mol}/\text{l}$ (31, 32).

¹³C-fatty acid modeling simulations

The model initial conditions were $C_R(0) = c_{ma}(0)$, with c_{ma} the maternal artery measurements (corresponding to the concentration in the reservoir R). The initial ¹³C-fatty acid concentrations in all other compartments were set at zero. The ¹³C-fatty acid amount used in the experiments were much lower than the metabolic K_m . Thus, equations 10 and 11 can be simplified:

$$J_{acc} = \frac{V_{max,acc} C_S}{K_{m,acc} + C_S} \approx \frac{V_{max,acc} C_S}{K_m} = k_{a,trac} C_S, \text{ for } K_m \gg C_S \quad (\text{Eq. } 12)$$

$$J_{rel} = \frac{V_{max,rel} C_P}{K_{m,rel} + C_P} \approx \frac{V_{max,rel} C_P}{K_m} = k_{r,trac} C_P, \text{ for } K_m \gg C_P \quad (\text{Eq. } 13)$$

where $k_{a,trac}$ (per minute) and $k_{r,trac}$ (per minute) are linear rate parameters, where the former represented the accumulation and the latter the release metabolic pathway.

Endogenous (unlabeled) fatty acid modeling simulations

The model initial conditions for the maternal and fetal compartment were $C_M(0) = c_{mv}(0)$ and $C_F(0) = c_{fv}(0)$, respectively, with c_{mv} the maternal vein measurements (representing the intervillous space M) and c_{fv} the fetal vein measurements (representing the fetal capillaries volume F). The initial concentration in the reservoir R was set to zero for most of the endogenous fatty acids, except for those that had been added in together with the ¹³C-fatty acid in the experiment at time zero (see MATERIALS AND METHODS). The initial syncytiotrophoblast concentration was $C_S(0) = (c_{mv}(0) + c_{fv}(0))/2$, as an estimated value according to the overall gradient expected at time 0. In addition, it was assumed that the endogenous pool was large, with $C_P(0) \gg K_m$ (33) and $C_P(0) \gg C_S(0)$. Thus, equations 10 and 11 can be simplified as:

$$J_{acc} = \frac{V_{max,acc} C_S}{K_{m,acc} + C_S} \approx \frac{V_{max,acc} C_S}{K_m} = k_{a,endo} C_S, \text{ for } K_m \gg C_S \quad (\text{Eq. } 14)$$

$$J_{rel} = \frac{V_{max,rel} C_P}{K_{m,rel} + C_P} \approx \frac{V_{max,rel} C_P}{C_P} = k_{r0,endo}, \text{ for } C_P \gg K_m \quad (\text{Eq. } 15)$$

where $k_{a,endo}$ (per minute) represents the accumulation metabolic pathway as a linear rate. $k_{r0,endo}$ ($\mu\text{mol}/\text{l}/\text{min}$) represents the endogenous metabolic release pathway as a constant rate.

Parameter estimation

The model parameter values are reported in **Table 1**, with mass (kg) of the perfused cotyledon equated to the approximate total volume V_{coty} in liters (24). Volumes of M , S , and F compartments were calculated based on volume fractions of 34, 15, and 7.5% of V_{coty} (24). The membrane dissociation constant K (equations 8 and 9) for different fatty acids were based on representative values from the literature (Table 1). The set of parameters to estimate was given by $p_{tra} = [v_{MVM}, v_{BM}, k_{a,tra}, k_{r,tra}]$ for the ¹³C-fatty acid and by $p_{endo} = [v_{MVM}, v_{BM}, k_{a,endo}, k_{r0,endo}]$ for the endogenous fatty acids. Considering the measurement $c_{k,i}$ for the k th compartment and the i th time point and $y_{k,i}$ as the model predictions for the k th compartment made at time i , the estimation of p was:

TABLE 1. Summary of the model parameter values

Parameter	Value	Unit	Description
V_R	0.20	liters	maternal reservoir volume
V_M	$0.34V_{coty}$	liters	intervillous space volume
$V_S = V_P$	$0.15V_{coty}$	liters	syncytiotrophoblast volume
V_F	$0.075V_{coty}$	liters	fetal capillaries volume
Q_M	0.0084	l/min	maternal circulation flow
Q_F	0.0040	l/min	fetal circulation flow
K	0.22	$\mu\text{mol}/\text{l}$	dissociation constant for saturated fatty acid (44–46)
K	0.18	$\mu\text{mol}/\text{l}$	dissociation constant for mono-unsaturated fatty acid (44, 46–50)
K	0.15	$\mu\text{mol}/\text{l}$	dissociation constant for poly-unsaturated fatty acid ($C < 20$) (44, 46, 51)
K	0.06	$\mu\text{mol}/\text{l}$	dissociation constant for very long-chain poly-unsaturated ($C \geq 20$) (46)
K_m	435	$\mu\text{mol}/\text{l}$	metabolic pool accumulation and release affinity constant (31, 32)

$$p_{\mathbf{x}} = \underset{p}{\arg \min} \sum_{k=1}^h \left[\sum_{i=1}^m (c_{k,i} - y_{k,i})^2 \right], \mathbf{x} = [\text{tra}, \text{endo}] \quad (\text{Eq. 16})$$

with $h = 3$ compartments and m the total number of time-points. Simulations and parameter estimations were implemented in MATLAB2015a (The MathWorks, Inc., Natick, MA). The governing model equations were integrated over time using Runge-Kutta 4th-5th (MATLAB: Ode45). The minimization of equation 16 was carried out using the Trust-Region-Reflective algorithm (MATLAB: lsqnonlin). The integrals of equations 1 and 2 were solved using the trapezoidal numerical integration (MATLAB: trapz).

Nonsaturable transport test

The impact of simple diffusion as opposed to a saturable transport process on the overall transfer of fatty acid across the placental membranes was evaluated by modifying the membrane fluxes from a saturable to a nonsaturated simple diffusive process. Thus:

$$J_{MVM} = q_{MVM} (C_M - C_S) \quad (\text{Eq. 17})$$

$$J_{BM} = q_{BM} (C_M - C_S) \quad (\text{Eq. 18})$$

where q_{MVM} and q_{BM} are the diffusion rate capacities of the membranes (l/min). In addition, a model was tested using the saturable form for J_{MVM} (equation 8) and simple diffusion for J_{BM} (equation 11).

Sensitivity analysis

The sensitivity analysis of the model was carried out in which each parameter was varied in turn while all others were kept fixed

at their reference values (either best-fit estimates or as given in Table 1) to evaluate the impact on the uptake and delivery for ^{13}C -fatty acid and the maternal and fetal recovery for endogenous fatty acids. An analysis of the controlling effects of the parameters and mechanisms affecting uptake and transfer in the system was carried out in which the MVM maximum rate v_{MVM} was varied over three orders of magnitude. For each fixed value of v_{MVM} , the other parameters were fitted according to the criterion in equation 14 to determine the impact on the quality of fit of different combinations of parameters.

Statistics

Statistical comparisons between two groups were performed using the unpaired t -test. Statistical analysis of comparison among multiple fatty acids was performed using one-way ANOVA (MATLAB: multcompare) with Turkey-Kramer post hoc correction. Statistical significance was assumed with when $P \leq 0.05$. Data are presented as mean values and SEM.

RESULTS

After an initial phase of approximately 10 min, the fetal vein concentrations reached a steady state, whereas maternal vein and reservoir concentrations gradually decreased for ^{13}C -fatty acid and increased for endogenous fatty acids over time (Fig. 2A). In addition, the washout phase showed a quick drop followed by another steady state both in maternal and fetal vein concentrations, in particular for the endogenous fatty acids (Fig. 2B).

The proportion of ^{13}C -fatty acid in the maternal reservoir taken up by the placenta was on average $61 \pm 10\%$, with no significant difference between fatty acid (Fig. 3A). The

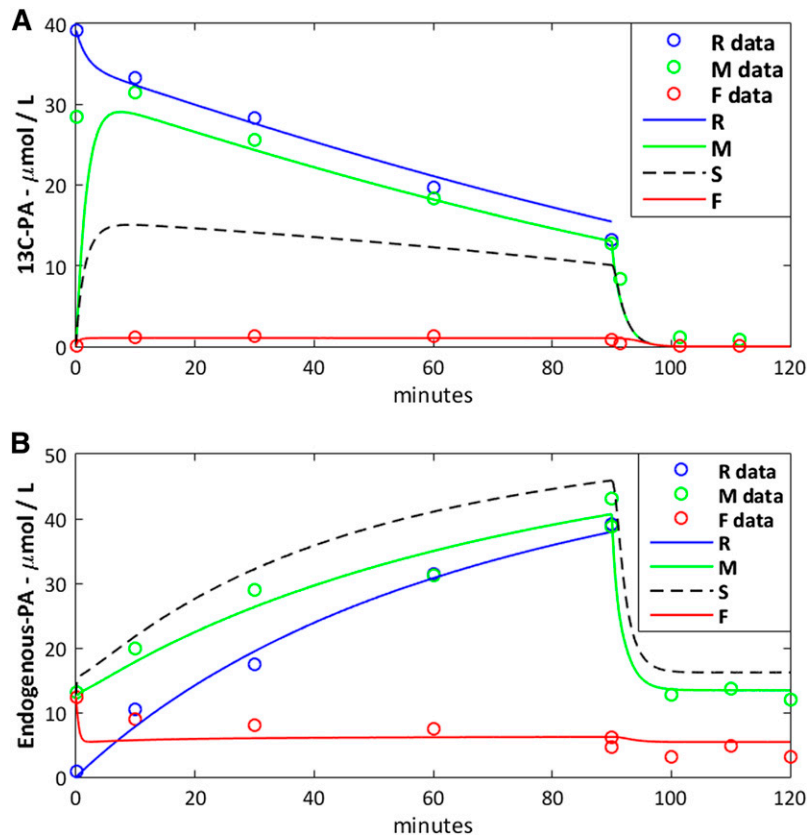


Fig. 2. Experimental data versus model prediction for palmitic acid. A: Data for the ^{13}C -palmitic acid (^{13}C -PA) added to the maternal reservoir. B: Data for the endogenous palmitic acid (C16:0) released from placental tissue. The experimental data are represented as hollow circles and the model predictions by solid and dashed lines. The syncytiotrophoblast prediction (S) is represented by a dashed line due to the lack of measurements available to compare with the model.

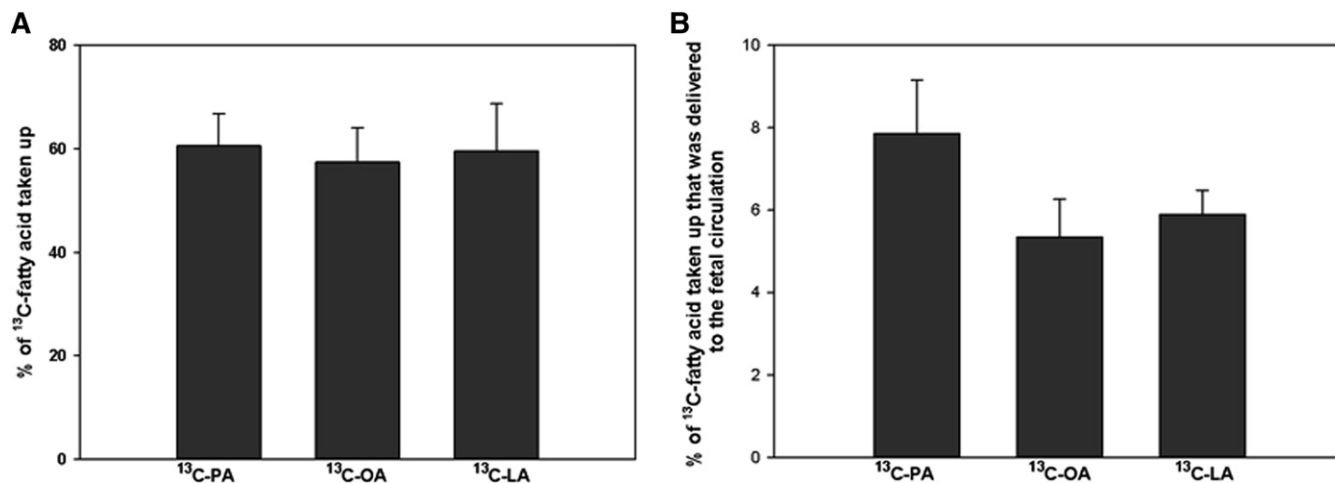


Fig. 3. Comparison of ¹³C-fatty acid uptake and transfer in the perfused placenta. A: ¹³C-fatty acid taken up by the placenta from the maternal circulation as a percentage of the amount initially present in the reservoir. B: ¹³C-fatty acid delivered to the fetal circulation as a percentage of the amount taken up by the placenta. ¹³C-LA, linoleic acid-labeled fatty acid; ¹³C-OA, oleic acid-labeled fatty acid; ¹³C-PA, palmitic acid-labeled fatty acid. No statistical differences were found. Data are expressed as mean \pm SEM (n = 6).

placental ¹³C-fatty acid mass balance b was greater than zero, and it was estimated that on average $93.8 \pm 0.8\%$ of the ¹³C-fatty acid taken up from the maternal circulation was retained in the placenta; the remaining $6.2 \pm 0.8\%$ was delivered to the fetal circulation (Fig. 3B), with no statistical differences between fatty acids.

The endogenous fatty acids mass balance b was greater than zero, demonstrating that a substantial net amount of fatty acid was released by the placenta into the circulations. On average, and summing both circulations, the measured amount of palmitic acid (C16:0) was the highest ($39 \pm 8\%$ of the total; $P < 0.05$), followed by linoleic acid (C18:2n6) ($26 \pm 8\%$), oleic acid (C18:1) ($14 \pm 4\%$), and arachidonic acid (C20:4n6) ($10 \pm 5\%$) (Fig. 4A). Excluding arachidonic acid and eicosapentaenoic acid, which had been added in the experiment, the average amount of endogenous fatty acid released from the placental tissue and recovered in the maternal circulation was $78 \pm 5\%$ of the total, and the remaining $22 \pm 5\%$ was found in the fetal circulation. This is reflected in the recovery of different endogenous fatty acids (Fig. 4B).

Modeling results

The model predictions were found to correspond well to the experimental data ($R^2 > 0.8$) (Fig. 2). The model could not fit the experimental data without the metabolic pool because the absence of metabolism would result in a 15-fold overprediction of the fetal delivery of ¹³C-fatty acids.

The parameter estimation results are summarized in Fig. 5A. For the ¹³C-fatty acid, the MVM rate capacity v_{MVM} was found to be much larger than v_{BM} on the BM by more than two orders of magnitude. The accumulation rate $k_{a,tra}$ was found similar among ¹³C-fatty acid with an average value of $0.9 \pm 0.1/\text{min}$ (results not shown). The release rate for ¹³C-fatty acid $k_{r,tra}$ was found to be 0 for all ¹³C-fatty acid. The results for the endogenous fatty acids are summarized in Fig. 5B, where the MVM maximum rate capacity was two orders of magnitude larger than that of the BM. The v_{MVM}

was higher for the palmitic acid (C16:0) and linoleic acid (C18:2n6) compared with the rest, except for oleic acid and arachidonic acid (C20:4n6) ($P < 0.01$). v_{BM} was higher for palmitic acid compared with the rest ($P < 0.01$). The accumulation pathway rate constant $k_{a,endo}$ for the metabolic pool was higher for α -linolenic acid (C18:3n3) compared with the rest, except dihomo- γ -linolenic acid (C20:3n6) and eicosapentaenoic acid (C20:5n3) ($P < 0.01$) (Fig. 6A). The release pathway rate constant $k_{r,endo}$ was the highest for palmitic acid (C16:0) ($P < 0.01$), whereas oleic acid (C18:1), linoleic acid (C18:2n6), and arachidonic acid (C20:4n6) were larger than the rest of the fatty acids ($P < 0.01$) (Fig. 6B).

Nonsaturable membrane transport

The modified model with both the MVM and BM membrane fluxes implemented as simple diffusive processes (using equations 17 and 18 instead of equations 8 and 9) could represent the experimental ¹³C-fatty acid data but failed to do so for the endogenous fatty acids. In particular, for the endogenous simulations, the “diffusive” model could not follow the fetal vein steady state and the washout phase (results not shown). Another “mixed” version of the model was evaluated in which the MVM flux was kept as a saturable mechanism (equation 8) and the BM as a simple diffusive process (equation 18). This model could not fit the endogenous fetal vein steady state (results not shown). Therefore, implementing simple diffusion as the sole mechanism in either membrane led to a worse fit of the data.

Parameter sensitivity analysis and fitting procedure

The model sensitivity analysis in Fig. 7A suggested that the uptake was sensitive to the metabolic pool accumulation rate $k_{a,tra}$ for the ¹³C-fatty acid. Delivery to the fetus was sensitive to changes in the fetal flow Q_f , the BM rate capacity v_{BM} , and the membrane parameter K . For the endogenous fatty acids in Fig. 7B, the sensitivity analysis showed

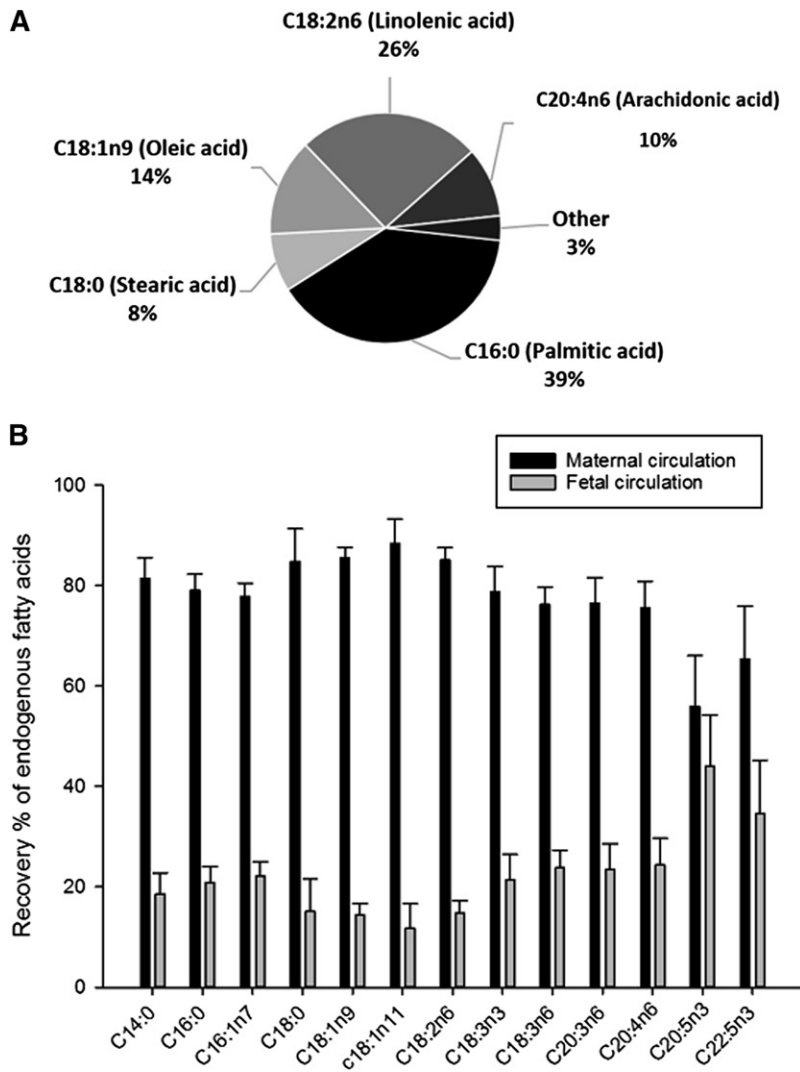


Fig. 4. The release of endogenous fatty acids from the perfused placenta: mass balance results ($t = 0-180$ min). A: Endogenous fatty acid release by the placenta. B: Percentages of the fatty acid release recovered in the maternal circulation and in the fetal circulation as part of the total released. Maternal recovery was significantly higher than fetal recovery for all fatty acids except C20:5n3 ($P < 0.01$). All values are expressed as mean \pm SEM ($n = 6$).

that the parameters that produced the largest effects on the absolute amount of fatty acid released to the maternal circulation were the metabolic incorporation and release parameters $k_{a,endo}$ and $k_{r,endo}$ and the reservoir volume V_R . The fetal delivery instead reported sensitivity for the v_{BM} , the metabolic accumulation rate $k_{a,endo}$, K , and Q_F . Similar results were found for the other ^{13}C -fatty acids (results not shown).

The ability of the model to explain the experimental data was investigated further by studying the interactions between different combinations of parameters (Fig. 8). v_{MVM} was varied while the other parameters were fitted according to equation 16, and the goodness-of-fit values of either the maternal or fetal data were reported as R^2 (red and orange lines). The maternal-side data represent the uptake process, and the fetal-side data represent the delivery. To the left of the vertical dashed line, the uptake could not be fitted because the membrane transport capacity v_{MVM} was too low to follow the experimental decrease in maternal concentrations over time observed in Fig. 2A (i.e., even for the maximum possible gradient across the MVM with syncytiotrophoblast concentrations C_s equal to zero). To the right, the uptake was fitted well irrespective of the increasing values of v_{MVM}

which was compensated for by an increase in syncytiotrophoblast concentrations C_s (lowering the MVM gradient) via a reduction in the metabolic accumulation rate parameter $k_{a,tr}$. Once the MVM uptake capacity was large enough, it was no longer limiting, and uptake was determined by the metabolic accumulation rate, which approached a constant value. The fetal delivery became well fitted toward the right when v_{BM} fluctuations stabilized once sufficiently high syncytiotrophoblast concentrations C_s were available for BM transport; further increases were irrelevant. The best fit (vertical dotted line) was found on the right side in this stable region. Thus, also considering that only 6.2% of the total tracer taken up by the placenta was delivered to the fetal circulation, fatty acid uptake was primarily controlled by the rate of incorporation into the metabolic pool, whereas the delivery was controlled by the combination of metabolic pool and BM rate capacity.

DISCUSSION

This study presents a mathematical model that is able to represent the experimental data for uptake and release

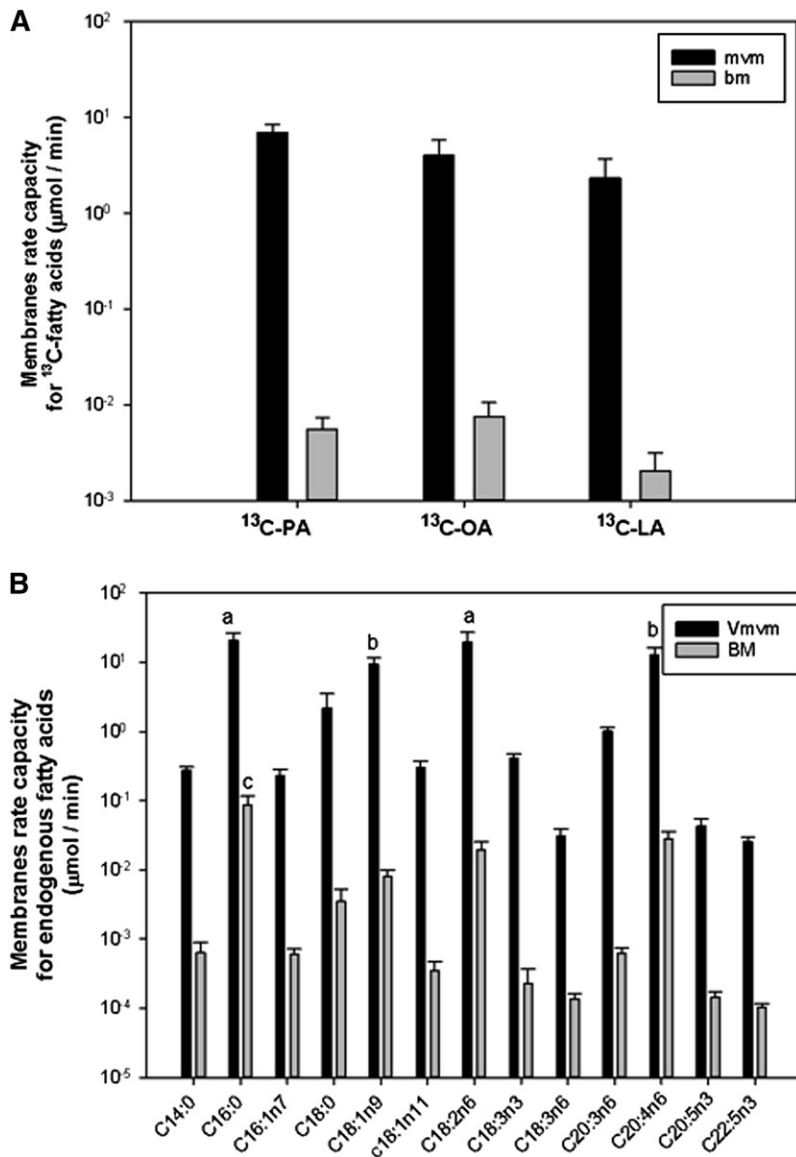


Fig. 5. Maximum transport rate model parameters for MVM and BM. A: ^{13}C -LA, linoleic acid-labeled fatty acid; ^{13}C -OA, oleic acid-labeled fatty acid; ^{13}C -PA, palmitic acid-labeled fatty acid. B: Endogenous fatty acids membrane rate capacities (marked with “a”) differed from the rest of the endogenous fatty acids except those marked with “b” ($P < 0.01$), which were not different from the rest of the substrates ($P < 0.05$). Fatty acids marked with “c” differed from the rest of the endogenous fatty acids ($P < 0.05$). All values are expressed as mean \pm SEM ($n = 6$).

of perfused exogenous ^{13}C -fatty acids and the unlabeled endogenous fatty acids. A key finding of the model was that when modeling membrane transport alone the model could not fit the experimental data because fetal delivery would be overpredicted by a factor of 15. In order for the model to work, it was necessary to model a separate metabolic pool representing all metabolic processes (i.e., incorporation of fatty acids into other lipid pools as well catabolism). The model supported higher permeability of the maternal side of the placenta to fatty acids compared with the fetal side. The model suggested that on the MVM the rates of the metabolic processes are dominant in determining fatty acid uptake, whereas both metabolic processes and basal membrane transport processes are rate determining for placental fatty acid transfer to the fetus.

Transport across placental membranes

The MVM was found to have a greater flux capacity than the BM based on both the experimental data and model

simulations. This was supported by the observation that 78% of all endogenous fatty acids recovered were found in the maternal reservoir even though this operated in closed circuit (which would reduce net transfer due to reuptake). The inequality between the MVM and BM membrane capacities could be due to differences in transport across the membrane, such as differences in transporter activity. However, it may also be due to factors that are not explicitly included in the model but that are bundled in the model parameter v , such as exchange area, diffusion across the stroma, and endothelial permeability. Similarly, the dissociation constant K used to represent the saturation process could implicitly account for the competition among fatty acids (i.e., apparent K_m is higher in the presence of competitive substrates). Increasing the flows in the maternal and fetal circulation was not predicted to influence placental fatty acid uptake, whereas fatty acid delivery to the fetus was predicted to be sensitive to the fetal blood flow (Fig. 7B). However, this modeling prediction needs to be tested by future experiments.

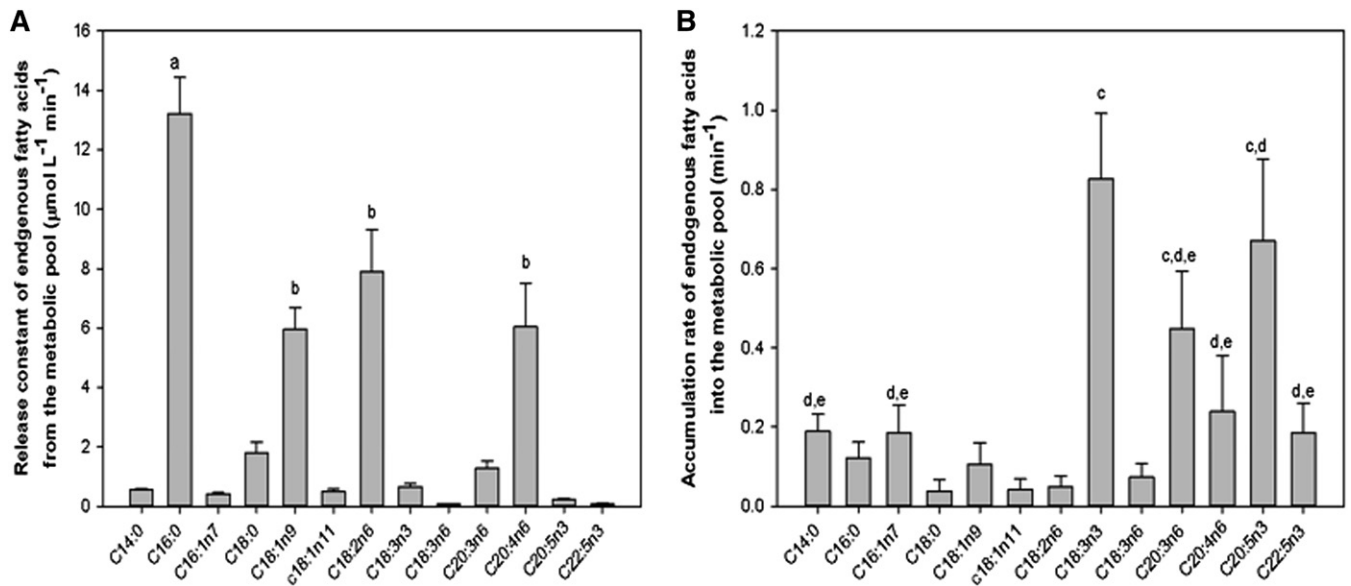


Fig. 6. Endogenous fatty acid model parameter estimation for the metabolic pool pathway. A: Metabolic pool release pathway rate constant ($k_{r,endo}$, $\mu\text{mol/L}/\text{min}$). The substrates labeled “a” differed from the rest of the endogenous fatty acids ($P < 0.01$). B: Metabolic pool accumulation pathway constant (k_a , per minute). Substrates labeled “a” differ from the rest of the endogenous fatty acids. Substrates labeled “b” differ from the rest of the endogenous fatty acids but not within the same group ($P < 0.01$). Substrates labeled “c,” “d,” and “e” differed from the rest of the endogenous fatty acids but not within the same group ($P < 0.01$). All values are expressed as mean \pm SEM ($n = 6$).

There were a number of assumptions within the model that are relevant to our understanding of the underlying physiological processes. Membrane transport of fatty acids was implemented within the model as a saturable process, without excluding the potential contribution of simple diffusion (which cannot be distinguished from facilitated transport in the linear regime). Although we could not distinguish between simple and facilitated diffusion for the ¹³C-fatty acid, the quality of fit was reduced when models based on pure simple diffusion were attempted for the endogenous fatty acids. The model did not distinguish between membrane transport kinetics and the kinetics of disassociation of insoluble fatty acids from binding proteins in the plasma or cytosol. Depending on the physiological or experimental system, the effects of albumin association and dissociation on fatty acid transfer may need to be taken into account explicitly (9, 12, 34, 35). Furthermore, other transport processes may exist, including active and selective transport systems (e.g., the recently discovered DHA transporter [36]) and endocytotic uptake of lipoproteins (37).

Placental metabolism determines uptake of maternal fatty acids

Our initial assumption was that the membrane transport would be the rate-determining factor for placental fatty acid uptake by the placenta. However, modeling of the experimental data suggests that fatty acid metabolism, not membrane transport, is the main rate-determining factor. This is because when membrane transport has a high capacity, the transmembrane gradient becomes small and metabolism becomes the rate-determining driver of uptake. A similar conclusion about the role of metabolism was reached in a study of fatty acid uptake into cardiac myocytes (12).

Placental metabolism may buffer the supply of fatty acids to the fetal circulation

In contrast to the maternal side of the placenta, on the fetal side the model predicts that both metabolism and membrane transport influence the supply of fatty acids to the fetus. This is because the placental-fetal transport capacity is lower than for maternal-placental transport. Although transport capacity is more important on the fetal side of the placenta, the driving force for fatty acid transport is still the transmembrane fatty acid gradient, which is determined by incorporation and release of fatty acids by the metabolic pool. We suggest that the metabolic pool may buffer the transfer of fatty acids to the fetal circulation. This is supported by our observations of a relatively constant steady state of the fetal vein fatty acid concentrations irrespective of variations in the maternal concentrations.

The washout phase of the experiment provides important support for the role of the metabolic pool and in particular the results for the endogenous fatty acids. When switched to open-circuit perfusion, the maternal vein concentration dropped quickly and stabilized at the same level as at the start of the experiment, when the maternal arterial input concentration from the reservoir was zero. This rapid drop, followed by a new equilibrium in output, is only possible if the intracellular concentration that is readily available for transport represents a very small fraction of the total fatty acid in the tissue (whether free or incorporated within more complex lipid classes). This is in accordance with a previous study in rat placenta, which estimated that, during materno to fetal transfer, fatty acids pass through a small placental compartment that accounts for only 5% of the total placental free fatty acid (38).

The fetal response during washout displays a similar drop and new equilibrium, whereas the only external

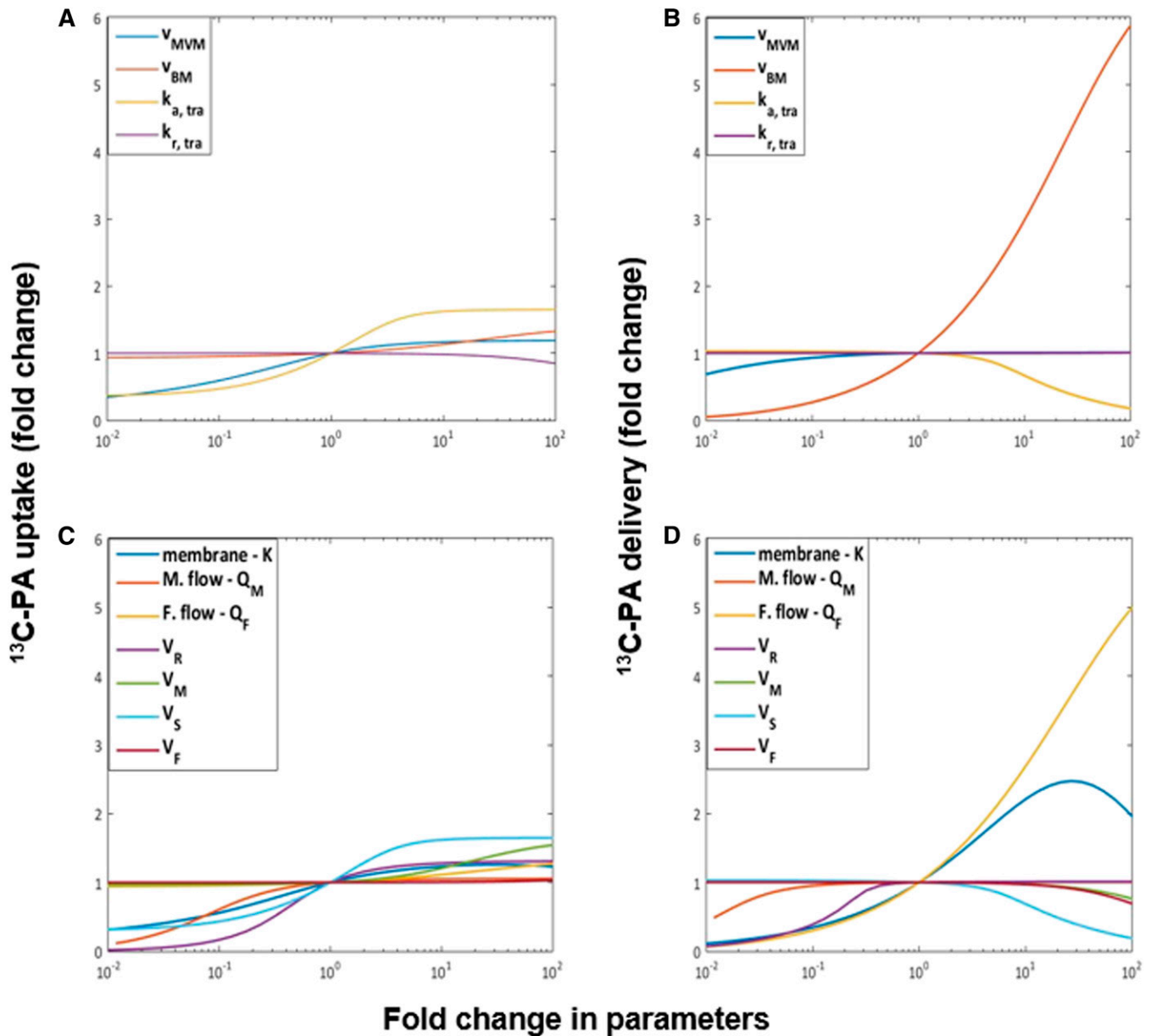


Fig. 7. Sensitivity analysis for the model parameters with respect to the total uptake and delivery of ^{13}C -palmitic acid (^{13}C -PA). The x axis represents the fold change in parameters compared with the reference values. v_{MVM} and v_{BM} are the maximum flux capacities of the MVM and BM, respectively. $k_{\text{a,tra}}$ and $k_{\text{r,tra}}$ are the accumulation and release rate constants for placental metabolism. K is the fatty acid membrane dissociation constant. Q_{M} and Q_{F} are the maternal and fetal flow rates. V_{R} , V_{M} , V_{S} , and V_{F} are the volumes of the reservoir, maternal intervillous, syncytiotrophoblast, and fetal capillary compartments, respectively. The y axis represents the change in the amount of either uptake or delivery of ^{13}C -PA. A: Analysis of the estimated parameters with respect to the uptake. B: Analysis of the model parameters with respect to the uptake. C: Analysis for the estimated parameters with respect to the delivery. D: Analysis of the estimated parameters with respect to the delivery.

change is the switch to open circuit perfusion on the maternal side. The explanation provided by the model is that the concentration of fatty acids available for transport in the syncytiotrophoblast drops rapidly due to the increased transport to the maternal side (most fatty acids diffuse out the maternal side because it is the route of least resistance), reducing the gradients driving BM transport. According to our model scheme, the internal concentrations available for transport are then sustained at a constant lower level by release from the metabolic pool, and this concentration determines the transport across the BM.

The model assumes the metabolic pool is located within the syncytiotrophoblast because this is in direct contact with the maternal plasma. However, we cannot exclude a role for other placental cell types, and a recent study has suggested a role for the cytotrophoblast in lipid metabolism (39). In the current study, we obtained an initial estimation of the metabolic activity in the placental tissue. Future studies are needed to determine specifically which lipid pools the fatty acids taken up by the placenta are incorporated into and the rate of β -oxidation of these fatty acids. This may be of clinical relevance because placental lipid metabolism is reported to be

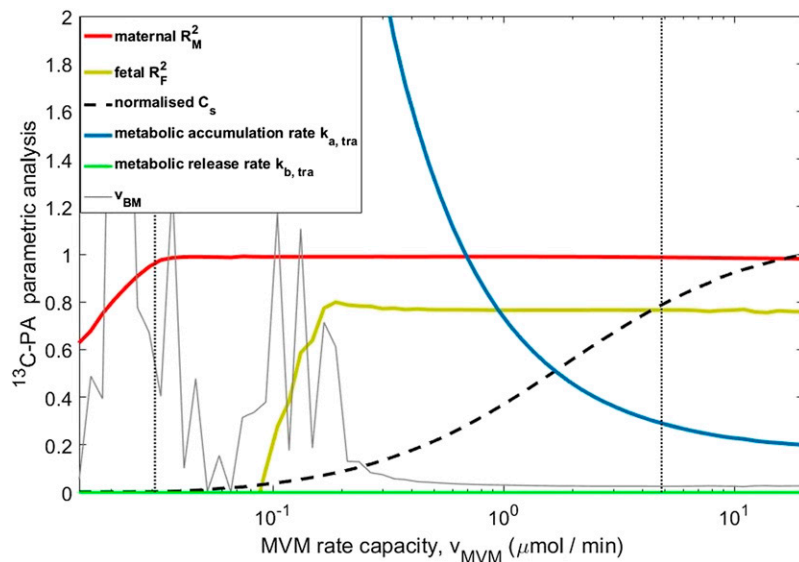


Fig. 8. Experimental data can be represented over a wide range of MVM transport capacities v_{MVM} , as long as the metabolic accumulation rate constant k_a is adjusted. Results for ^{13}C -PA are shown. The MVM rate capacity v_{MVM} (x axis) was varied over a range of fixed values, and the other unknown parameters were fitted again for each value of v_{MVM} to best represent the data. The red and yellow lines indicate the R^2 for the maternal-side concentrations and fetal-side concentrations after the initial phase ($t \geq 10$ min). The left vertical line (dashed) is the minimum value of v_{MVM} below which the experimental uptake could not be represented (see text). The right vertical black line (dotted) indicates the best fit found previously. Higher values of v_{MVM} tend to equalize the maternal and syncytiotrophoblast fatty acid concentrations in the model (C_s normalized by the maternal vein measurement at 90 min of perfusion). This implies that for high v_{MVM} uptake is only determined by k_{tr} , which approaches a constant value. Results are similar for the other fatty acids. The fluctuations in v_{BM} on the left are because this parameter cannot be fitted if the syncytiotrophoblast concentrations available for transport C_s are too low.

altered in diabetic pregnancy (40, 41). Although the perfused placenta is a highly useful model, it must be remembered that there will be many differences in vivo, including the concentrations of maternal and fetal substrates and hormones, which may both influence placental metabolism and transport. Furthermore, in the perfusion model, the total availability of fatty acids to the placenta are lower than in vivo because we only perfused with a limited number of fatty acids and therefore there will not be any release of fatty acids from lipoproteins. Lower fatty acid availability could have influenced the proportion of fatty acids entering the metabolic pool; therefore, the metabolic capacity of this pool needs to be investigated further.

Differences between fatty acids

There is preferential transfer of specific long-chain PUFAs across the placenta, which is referred to as “biomagnification” (42). It has been assumed that this is due to preferential transport of long-chain PUFAs, but it may be that differential metabolism underlies this process. The estimated endogenous MVM and BM membrane transport capacities and metabolic rate parameters in the model displayed considerable variation between fatty acids. The accumulation rate parameters in the model displayed the highest values for α -linolenic acid (C18:3n3) and eicosapentaenoic acid (C20:5n3), which, in combination with release, could indicate a tighter metabolic control of their syncytiotrophoblast concentrations for these omega-3 fatty acids. This is in accordance with results of a recent cohort study in which the portions of linoleic acid and α -linolenic acid as long-chain precursors were lower in fetal than in maternal plasma (43), supporting our idea that the metabolic pool may buffer the transfer of specific fatty acids to the fetal circulation. These estimated parameters clearly indicate biological variation in the underlying processes but should not be overinterpreted because they incorporate a range of factors not explicitly captured within the model.

Conclusion

In summary, a combined computational-experimental approach was adopted, highlighting the importance of the metabolic pool in the placental transfer of fatty acid. We propose that fatty acid uptake is regulated by metabolism rather than microvillous membrane transport and that delivery of fatty acids to the fetus is determined by both metabolism and basal membrane transfer. The modeling framework can be extended further in the future as new data become available to describe in more detail the metabolic pathways and transport mechanisms involved, including interactions and competition between fatty acids, which were not included in this study. In particular, this should be informed by more detailed experimental analysis of metabolic subcompartments in placental tissue. [DOI](#)

REFERENCES

- Larqué, E., A. Pagán, M. T. Prieto, J. E. Blanco, A. Gil-Sánchez, M. Zornoza-Moreno, M. Ruiz-Palacios, A. Gázquez, H. Demmelmair, and J. J. Parrilla. 2014. Placental fatty acid transfer: a key factor in fetal growth. *Ann. Nutr. Metab.* **64**: 247–253.
- Lewis, R., H. Demmelmair, R. Gaillard, K. Godfrey, S. Hauguel-de Mouzon, B. Huppertz, E. Larque, R. Saffery, M. Symonds, and G. Desoye. 2013. The placental exposome: placental determinants of fetal adiposity and postnatal body composition. *Ann. Nutr. Metab.* **63**: 208–215.
- Dancis, J., V. Jansen, and M. Levitz. 1976. Transfer across perfused human placenta: IV. Effect of protein binding on free fatty acids. *Pediatr. Res.* **10**: 5–10.
- Richieri, G. V., R. T. Ogata, and A. M. Kleinfeld. 1996. Kinetics of fatty acid interactions with fatty acid binding proteins from adipocyte, heart, and intestine. *J. Biol. Chem.* **271**: 11291–11300.
- Vork, M. M., J. Glatz, and G. Van der Vusse. 1997. Modelling intracellular fatty acid transport: possible mechanistic role of cytoplasmic fatty acid-binding protein. *Prostaglandins Leukot. Essent. Fatty Acids.* **57**: 11–16.
- Haggarty, P. 2010. Fatty acid supply to the human fetus. *Annu. Rev. Nutr.* **30**: 237–255.

7. Lager, S., and T. L. Powell. 2012. Regulation of nutrient transport across the placenta. *J. Pregnancy*. **2012**: 179827.
8. Kamp, F., and J. A. Hamilton. 2006. How fatty acids of different chain length enter and leave cells by free diffusion. *Prostaglandins Leukot. Essent. Fatty Acids*. **75**: 149–159.
9. Glatz, J. F. 2015. Lipids and lipid binding proteins: a perfect match. *Prostaglandins Leukot. Essent. Fatty Acids*. **93**: 45–49.
10. Lager, S., V. I. Ramirez, F. Gaccioli, B. Jang, T. Jansson, and T. L. Powell. 2016. Protein expression of fatty acid transporter 2 is polarized to the trophoblast basal plasma membrane and increased in placentas from overweight/obese women. *Placenta*. **40**: 60–66.
11. Cunningham, P., and L. McDermott. 2009. Long chain PUFA transport in human term placenta. *J. Nutr.* **139**: 636–639.
12. Luiken, J. J., F. Van Nieuwenhoven, G. America, G. Van der Vusse, and J. Glatz. 1997. Uptake and metabolism of palmitate by isolated cardiac myocytes from adult rats: involvement of sarcolemmal proteins. *J. Lipid Res.* **38**: 745–758.
13. Araújo, J. R., A. Correia-Branco, C. Ramalho, E. Keating, and F. Martel. 2013. Gestational diabetes mellitus decreases placental uptake of long-chain polyunsaturated fatty acids: involvement of long-chain acyl-CoA synthetase. *J. Nutr. Biochem.* **24**: 1741–1750.
14. Faergeman, N. J., and J. Knudsen. 1997. Role of long-chain fatty acyl-CoA esters in the regulation of metabolism and in cell signaling. *Biochem. J.* **323**: 1–12.
15. Larqué, E., H. Demmelmair, B. Berger, U. Hasbargen, and B. Koletzko. 2003. In vivo investigation of the placental transfer of 13C-labeled fatty acids in humans. *J. Lipid Res.* **44**: 49–55.
16. Pathmaperuma, A. N., P. Mana, S. Cheung, K. Kugathas, A. Josiah, M. Koina, A. Broomfield, V. Delghingaro-Augusto, D. Ellwood, and J. Dahlstrom. 2010. Fatty acids alter glycerolipid metabolism and induce lipid droplet formation, syncytialisation and cytokine production in human trophoblasts with minimal glucose effect or interaction. *Placenta*. **31**: 230–239.
17. Shekhawat, P., M. J. Bennett, Y. Sadovsky, D. M. Nelson, D. Rakheja, and A. W. Strauss. 2003. Human placenta metabolizes fatty acids: implications for fetal fatty acid oxidation disorders and maternal liver diseases. *Am. J. Physiol. Endocrinol. Metab.* **284**: E1098–E1105.
18. Rakheja, D., M. Bennett, B. Foster, R. Domiati-Saad, and B. Rogers. 2002. Evidence for fatty acid oxidation in human placenta, and the relationship of fatty acid oxidation enzyme activities with gestational age. *Placenta*. **23**: 447–450.
19. Kuhn, D. C., and M. Crawford. 1986. Placental essential fatty acid transport and prostaglandin synthesis. *Prog. Lipid Res.* **25**: 345–353.
20. Day, P. E., J. Cleal, E. Lofthouse, M. Hanson, and R. Lewis. 2013. What factors determine placental glucose transfer kinetics? *Placenta*. **34**: 953–958.
21. Barrett, H. L., M. H. Kubala, K. S. Romero, K. J. Denny, T. M. Woodruff, H. D. McIntyre, L. K. Callaway, and M. D. Nitert. 2014. Placental lipases in pregnancies complicated by gestational diabetes mellitus (GDM). *PLoS One*. **9**: e104826.
22. Herrera, E., and G. Desoye. 2016. Maternal and fetal lipid metabolism under normal and gestational diabetic conditions. *Horm. Mol. Biol. Clin. Invest.* **26**: 109–127.
23. Lofthouse, E. M., S. Perazzolo, S. Brooks, I. P. Crocker, J. D. Glazier, E. D. Johnstone, N. Panitchob, C. P. Sibley, K. L. Widdows, and B. G. Sengers. 2015. Phenylalanine transfer across the isolated perfused human placenta: an experimental and modelling investigation. *Am. J. Physiol. Regul. Integr. Comp. Physiol.* **10**: R828–R836.
24. Sengers, B. G., C. P. Please, and R. M. Lewis. 2010. Computational modelling of amino acid transfer interactions in the placenta. *Exp. Physiol.* **95**: 829–840.
25. Panitchob, N., R. Lewis, and B. Sengers. 2016. Computational modelling of placental amino acid transfer as an integrated system. *Biochim. Biophys.* **1858**: 1451–1461.
26. Schneider, H., and A. Huch. 1985. Dual in vitro perfusion of an isolated lobe of human placenta: method and instrumentation. *Contrib. Gynecol. Obstet.* **13**: 40–47.
27. Matyash, V., G. Liebisch, T. V. Kurzchalia, A. Shevchenko, and D. Schwudke. 2008. Lipid extraction by methyl-tert-butyl ether for high-throughput lipidomics. *J. Lipid Res.* **49**: 1137–1146.
28. Fuchs, C. D., T. Claudel, P. Kumari, G. Haemmerle, M. J. Pollheimer, T. Stojakovic, H. Scharnagl, E. Halilbasic, J. Gumhold, and D. Silbert. 2012. Absence of adipose triglyceride lipase protects from hepatic endoplasmic reticulum stress in mice. *Hepatology*. **56**: 270–280.
29. Hanebutt, F. L., H. Demmelmair, B. Schiessl, E. Larqué, and B. Koletzko. 2008. Long-chain polyunsaturated fatty acid (LC-PUFA) transfer across the placenta. *Clin. Nutr.* **27**: 685–693.
30. Panitchob, N., K. Widdows, I. Crocker, M. A. Hanson, E. Johnstone, C. Please, C. Sibley, J. Glazier, R. Lewis, and B. G. Sengers. 2015. Computational modelling of amino acid exchange and facilitated transport in placental membrane vesicles. *J. Theor. Biol.* **365**: 352–364.
31. Kilbane, A. J., T. Petroff, and W. W. Weber. 1991. Kinetics of acetyl CoA: arylamine N-acetyltransferase from rapid and slow acetylator human liver. *Drug Metab. Dispos.* **19**: 503–507.
32. Boston, R. C., and P. J. Moate. 2008. A novel minimal model to describe NEFA kinetics following an intravenous glucose challenge. *Am. J. Physiol. Regul. Integr. Comp. Physiol.* **294**: R1140–R1147.
33. Pagán, A., M. T. Prieto-Sánchez, J. E. Blanco-Carnero, A. Gil-Sánchez, J. J. Parrilla, H. Demmelmair, B. Koletzko, and E. Larque. 2013. Materno-fetal transfer of docosahexaenoic acid is impaired by gestational diabetes mellitus. *Am. J. Physiol. Endocrinol. Metab.* **305**: E826–E833.
34. Arts, T., R. S. Reneman, J. B. Bassingthwaite, and G. J. van der Vusse. 2015. Modeling fatty acid transfer from artery to cardiomyocyte. *PLOS Comput. Biol.* **11**: e1004666.
35. Richieri, G. V., and A. M. Kleinfeld. 1995. Unbound free fatty acid levels in human serum. *J. Lipid Res.* **36**: 229–240.
36. Prieto-Sánchez, M. T., M. Ruiz-Palacios, J. E. Blanco-Carnero, A. Pagan, C. Hellmuth, O. Uhl, W. Peissner, A. J. Ruiz-Alcaraz, J. J. Parrilla, and B. Koletzko. 2016. Placental MFS2a transporter is related to decreased DHA in cord blood of women with treated gestational diabetes. *Clin. Nutr.* pii: S0261-5614(16)00036-4.
37. Malassine, A., C. Besse, A. Roche, E. Alsat, R. Rebourcet, F. Mondon, and L. Cedard. 1987. Ultrastructural visualization of the internalization of low density lipoprotein by human placental cells. *Histochemistry*. **87**: 457–464.
38. Hummel, L., T. Zimmermann, W. Schirrmeister, and H. Wagner. 1976. Synthesis, turnover and compartment analysis of the free fatty acids in the placenta of rats. *Acta Biol. Med. Ger.* **35**: 1311–1316.
39. Kolahi, K., S. Louey, O. Varlamov, and K. Thornburg. 2016. Real-time tracking of BODIPY-C12 long-chain fatty acid in human term placenta reveals unique lipid dynamics in cytotrophoblast cells. *PLoS One*. **11**: e0153522.
40. Kuhn, D. C., M. A. Crawford, M. J. Stuart, J. J. Botti, and L. M. Demers. 1990. Alterations in transfer and lipid distribution of arachidonic acid in placentas of diabetic pregnancies. *Diabetes*. **39**: 914–918.
41. Visiedo, F., F. Bugatto, V. Sánchez, I. Cozar-Castellano, J. L. Bartha, and G. Perdomo. 2013. High glucose levels reduce fatty acid oxidation and increase triglyceride accumulation in human placenta. *Am. J. Physiol. Endocrinol. Metab.* **305**: E205–E212.
42. Crawford, M. 2000. Placental delivery of arachidonic and docosahexaenoic acids: implications for the lipid nutrition of preterm infants. *Am. J. Clin. Nutr.* **71**: 275S–284S.
43. Schlörmann, W., R. Kramer, A. Lochner, C. Rohrer, E. Schlessner, G. Jahreis, and K. Kuhnt. 2015. Foetal cord blood contains higher portions of n-3 and n-6 long-chain PUFA but lower portions of trans C18: 1 isomers than maternal blood. *Food Nutr. Res.* **59**: 29348.
44. Abumrad, N., J. Park, and C. Park. 1984. Permeation of long-chain fatty acid into adipocytes. *J. Biol. Chem.* **14**: 1945–1953.
45. Trotter, P. J., S. Y. Ho, and J. Storch. 1996. Fatty acid uptake by Caco-2 human intestinal cells. *J. Lipid Res.* **37**: 336–346.
46. Neufeld, E., D. Wilson, H. Sprecher, and P. Majerus. 1983. High affinity esterification of eicosanoid precursor fatty acids by platelets. *J. Clin. Invest.* **72**: 214.
47. Schwieterman, W., D. Sorrentino, B. Potter, J. Rand, C. Kiang, D. Stump, and P. Berk. 1988. Uptake of oleate by isolated rat adipocytes is mediated by a 40-kDa plasma membrane fatty acid binding protein closely related to that in liver and gut. *Proc. Natl. Acad. Sci. USA*. **85**: 359–363.
48. Storch, J., C. Lechene, and A. M. Kleinfeld. 1991. Direct determination of free fatty acid transport across the adipocyte plasma membrane using quantitative fluorescence microscopy. *J. Biol. Chem.* **266**: 13473–13476.
49. Stremmel, W., G. Strohmeyer, and P. D. Berk. 1986. Hepatocellular uptake of oleate is energy dependent, sodium linked, and inhibited by an antibody to a hepatocyte plasma membrane fatty acid binding protein. *Proc. Natl. Acad. Sci. USA*. **83**: 3584–3588.
50. Stremmel, W. 1988. Fatty acid uptake by isolated rat heart myocytes represents a carrier-mediated transport process. *J. Clin. Invest.* **81**: 844.
51. Xu, Y., T. J. Cook, and G. T. Knipp. 2006. Methods for investigating placental fatty acid transport. *Methods Mol. Med.* **122**: 265–284.